AIMS Mathematics, 11(11): 39498–39522.
DOI: 10.3934/math.20261521
Received: 03 October 2026
Revised: 10 November 2026
Accepted: 16 November 2026
Published: 26 November 2026

https://www.aimspress.com/journal/Math

Research article

Event-triggered resilient consensus of heterogeneous multi-agent systems under inconsistent semi-Markov switching and composite attacks

Dongxiao Hu, Jiwei Gao*, Jianwei Ma, and Shaofei Zang

School of Information Engineering, Henan University of Science and Technology, Luoyang 471023, China

* **Correspondence:** Email: jwgao2012@163.com.

Abstract: This paper investigated resilient consensus control for heterogeneous multi-agent systems subject to inconsistent semi-Markov switching topologies and composite attacks. Inconsistent semi-Markov processes were introduced to characterize the stochastic switching communication topologies among agents with different dynamics. Furthermore, a composite attack model was constructed to capture simultaneous malicious attacks on sensor measurement and actuator control channels. Moreover, to reduce communication frequency and alleviate the adverse effects of instantaneous error fluctuations, a dual accumulative-error-based event-triggered mechanism was introduced. Based on this mechanism, a distributed secure consensus protocol was designed to enable secure cooperative control of all agents. By employing a stochastic analysis technique, Lyapunov stability theory, and some inequality techniques, sufficient conditions were derived to guarantee secure consensus of the closed-loop system. Finally, simulation results demonstrated that the proposed method can maintain consensus under composite attacks while effectively reducing the number of communication updates.

Keywords: resilient consensus; heterogeneous multi-agent systems; semi-Markov switching; composite attacks; accumulative-error-based event-triggered mechanism
Mathematics Subject Classification: 93A16, 93D50, 93C30

1. Introduction

Multi-agent systems (MASs) are distributed cooperative systems consisting of numerous agents communicating through local information exchange. Owing to their flexible architecture, strong robustness, and high scalability, MASs have been widely applied in unmanned aerial vehicle formations [1], cooperative robotics [2, 3], sensor networks [4], and intelligent transportation systems [5]. Multi-agent systems have also been studied in terms of their collective learning dynamics [6]. As one of the fundamental problems in MASs, consensus control aims to achieve

coordination, synchronization, or tracking among agents based on local neighborhood information. Therefore, it has remained an important research topic and has yielded numerous results [7, 8]. Most of these studies are based on homogeneous MASs, namely, where all agents have the same or similar dynamic behaviors. However, in practical engineering systems, agents often exhibit different characteristics due to variations in their physical structures, load conditions, and operating environments. For example, in cooperative tasks involving heterogeneous unmanned systems, unmanned ground vehicles (UGVs) and unmanned aerial vehicles (UAVs) may exhibit distinct dynamic characteristics [9, 10]. Therefore, consensus control of heterogeneous MASs (HMASs) can more accurately reflect the actual characteristics of complex engineering systems.

Meanwhile, the communication topology of MASs is susceptible to variations in network conditions and external disturbances, resulting in stochastic switching behavior. To characterize its stochastic evolution, Markov processes are introduced to model stochastic switching communication topologies [11–13]. However, the sojourn time of a communication topology does not necessarily follow an exponential distribution, and the mode transition probabilities may vary with time and environmental conditions. To characterize the stochastic switching process more accurately, semi-Markov processes are employed to describe more general sojourn-time distributions, such as the Weibull distribution [14]. In recent years, topology switching governed by semi-Markov processes has also gradually attracted attention, and some results have been achieved [15, 16]. Furthermore, since different agents may operate under different network environments and communication conditions, their topology switching behaviors are generally not identical. Therefore, an inconsistent semi-Markov process is employed to describe the switching topologies among agents. Specifically, different agents may follow semi-Markov processes with distinct sojourn-time distributions and transition laws, enabling a more accurate characterization of the stochastic switching characteristics of the communication topology.

In addition, when HMASs operate over open or semi-open communication networks, they are vulnerable to malicious attacks. Attackers may disrupt normal system operation through denial-of-service attacks [17], deception attacks [18], and false-data injection attacks [19]. However, compared to system faults [20], attack behaviors are often composite and stealthy. Existing studies on secure consensus mainly focus on a single type of attack, such as communication-link attacks [21], sensor attacks [22], or actuator attacks [23]. Attackers may tamper with sensor measurements, causing the controller to obtain erroneous state information. They may also directly act on actuator channels, alter the actual control inputs of the system, and weaken or even distort the control action. When these two types of attacks occur simultaneously, the system is subjected to the dual effects of inaccurate state estimation and distorted control inputs [24]. Therefore, jointly considering sensor and actuator attacks in HMASs is more consistent with practical secure control requirements and presents greater research challenges.

On the other hand, event-triggered mechanism (ETM) has been widely adopted in HMASs to reduce communication burdens and save network resources. Unlike conventional periodic sampling, ETM updates control signals or transmits state information only when predefined triggering conditions are satisfied, thereby effectively reducing unnecessary information exchange and control updates [25, 26]. Based on their threshold-update strategies, existing ETMs can generally be classified into static [27], dynamic [28], and adaptive mechanisms [29]. However, conventional ETMs typically compare the instantaneous measurement error with a prescribed threshold, making them susceptible

to instantaneous error fluctuations. To address this, an accumulative-error-based ETM (ABETM) is proposed in [30], in which the error is accumulated from the most recent triggering instant to the current instant, and an update is triggered once the accumulated error exceeds a specified threshold. Inspired by this approach, the ABETM is introduced into HMASs to avoid excessively long update intervals under small error fluctuations while maintaining a low triggering frequency.

Following the analysis presented above, this paper investigates secure control for HMASs subject to attacks under inconsistent semi-Markov switching topologies. By introducing an ABETM, a resilient controller is designed that ensures system security and consensus while reducing unnecessary communication updates. The main novelties and contributions of this work can be summarized as follows:

(i) A class of HMASs with inconsistent stochastic switching topologies is considered. Unlike existing studies on homogeneous MASs [6, 31] and identical Markov switching [13, 32], this paper investigates a system composed of first-order and second-order agents. Furthermore, an inconsistent semi-Markov process is adopted to characterize the topology switching of different agent types, which allows different agents to have distinct transition rules and sojourn-time distributions.

(ii) For composite attacks involving simultaneous sensor and actuator attacks, a secure control model is established for the HMASs under attack. Unlike studies that consider only sensor attacks [33] or actuator attacks [34], this paper simultaneously characterizes the effects of both types of attacks on state measurements and control inputs, thereby providing a more realistic representation of the complexity and stealthiness of attack behaviors in practical systems.

(iii) To reduce communication frequency and minimize the burden of control updates, a double ABETM is introduced, inspired by [30]. Unlike conventional schemes that rely on instantaneous errors, the proposed mechanism considers the accumulated error between two events. Data transmission occurs only when the accumulated error satisfies a prescribed threshold. This approach can reduce frequent triggering caused by instantaneous fluctuations and improve the efficiency of communication resource utilization while ensuring safety and consensus.

Notations: $\otimes$ denotes the Kronecker product. $*$ represents the terms omitted by symmetry. $\mathcal{F}^{-1}$ and $\mathcal{F}^{\mathrm{T}}$ denote the inverse and transpose of matrix $\mathcal{F}$, respectively. $\mathscr{I}_l$ is defined as the l-dimensional identity matrix. For simplicity, the time parameter t is omitted in this paper, such as $x_i = x_i(t)$. In addition, the following equation is: $\ell \triangleq \ell(t-\eta)$, where $\ell = x_i, v_i, \delta_{xi}, \delta_{vi}$, and the details will be explained later.

2. Preliminaries

2.1. Graph theory

In this paper, graph $\mathcal{G}^\sigma = (N, \mathcal{E}^\sigma, A^\sigma)$ represents a directed graph with n nodes, where $N = \{1, ..., n\}$ denotes the node set, $\mathcal{E}^\sigma$ is the edge set, and A^σ stands for the adjacent matrix. If agent i can communicate with agent j, then the edge $e_{ij}^\sigma \in \mathcal{E}^{\sigma_1}$ and $a_{ij} > 0$. Furthermore, defining the degree matrix $\mathcal{D} = \mathrm{diag}\{d_1, d_2, ..., d_n\}$ with $d_i = \sum_{j \in \mathcal{N}_i} a_{ij}^{\sigma_1(t)}$. The Laplacian matrix $L = \left(l_{ij}^{\sigma_1(t)}\right) \in \mathcal{R}^{n \times n}$ is defined

by $L = \mathcal{D} - A$ can be characterized as:

$$l_{ij}^{\sigma_1(t)} = \begin{cases} -a_{ij}^{\sigma_1(t)}, & j \neq i, \\ \sum\limits_{j=1, j\neq i}^{n} a_{ij}^{\sigma_1(t)}, & j = i. \end{cases}$$

Assumption 1. *For each admissible joint switching mode $(i, h) \in S_1 \times S_2$, the corresponding communication graph $\mathcal{G}^{i,h}$ contains a directed spanning tree. Accordingly, the associated Laplacian matrix $L^{i,h}$ has a simple zero eigenvalue, while all its other eigenvalues have positive real parts.*

2.2. System model

In this paper, a class of HMASs models involving both first-order and second-order agents is presented:

$$\begin{cases} \begin{cases} \dot{x}_i = u_i^c, \\ y_{xi} = x_i^c, \end{cases} & i \in N_1, \\ \begin{cases} \dot{x}_i = v_i, \\ \dot{v}_i = u_i^c, \\ y_{xi} = x_i^c, \\ y_{vi} = v_i^c, \end{cases} & i \in N_2, \end{cases} \tag{2.1}$$

where $N_1 = \{1, 2, ..., m\}$, $N_2 = \{m + 1, m + 2, ..., n\}$, which means that the HMASs (2.1) consists of m first-order agents and $n - m$ second-order agents. x_i and v_i denote the state and velocity variables of agent i, respectively. y_{xi} and y_{vi} represent the measurement outputs affected by the sensor attack, respectively. u_i^c denotes the control input affected by the actuator attack.

Assume that the communication topology among agents in HMASs (2.1) follows an inconsistent semi-Markov process, implying that agents of different orders follow different semi-Markov processes. Let $\sigma_1(t)(t > 0)$ denote a continuous-time semi-Markov process with right-continuous trajectory, taking values in a finite set $S_1 = \{1, ..., s_1\}$. The transition probability is defined as:

$$P_1\{\sigma_1(t + \Delta t) = \varphi | \sigma_1(t) = \phi, \tau_1(t) = \tau_1\} = \begin{cases} \pi_{\phi\varphi}^{(1)}(\tau_{1\phi})\Delta t + o(\Delta t), & \phi \neq \varphi, \\ 1 + \pi_{\phi\phi}^{(1)}(\tau_{1\phi})\Delta t + o(\Delta t), & \phi = \varphi, \end{cases}$$

where $\lim\limits_{\Delta t \to 0} (o(\Delta t)/\Delta t) = 0$ with $\Delta t > 0$. $\pi_{\phi\varphi}^{(1)}(\tau_{1\phi})$ represents the transition rate from mode ϕ to mode φ, and when $\phi = \varphi$, $\pi_{\phi\phi}(\tau) = -\sum_{\varphi \neq \phi} \pi_{\phi\varphi}(\tau)$. $\tau_{1\phi}$ denotes the residence time of the current mode. $\sigma_2(t)(t > 0)$ represents another continuous-time semi-Markov process with a finite value set $S_2 = \{1, ..., s_2\}$. Its transition probabilities are given by

$$P_2\{\sigma_2(t + \Delta t) = k \mid \sigma_2(t) = h, \tau_2(t) = \tau_2\} = \begin{cases} \pi_{hk}^{(2)}(\tau_2)\Delta t + o(\Delta t), & h \neq k, \\ 1 + \pi_{hh}^{(2)}(\tau_2)\Delta t + o(\Delta t), & h = k, \end{cases}$$

where $\tau_2(t)$ denotes the elapsed sojourn time of the current mode of $\sigma_2(t)$, and $\pi_{hk}^{(2)}(\tau_2)$ denotes the corresponding transition rate, satisfying $\pi_{hk}^{(2)}(\tau_2) \geq 0, h \neq k, \pi_{hh}^{(2)}(\tau_2) = -\sum_{k \neq h} \pi_{hk}^{(2)}(\tau_2)$.

The two semi-Markov processes, $\sigma_1(t)$ and $\sigma_2(t)$, are shared by the first-order and second-order agent groups, respectively, rather than being assigned individually to each agent. Specifically, all

agents in $\mathcal{N}_1$ follow $\sigma_1(t)$, while those in $\mathcal{N}_2$ follow $\sigma_2(t)$, allowing the two groups to exhibit different stochastic switching behaviors.

The relationship between $\sigma_1(t)$ and $\sigma_2(t)$ can be characterized by a known conditional probability matrix, defined as follows:

$$P_r\{\sigma_2(t) = h|\sigma_1(t) = i\} = \rho_{ih}.$$

Remark 1. *The main difference between Markov switching and semi-Markov switching lies in their sojourn-time characteristics. In conventional continuous-time Markov switching, the sojourn times follow exponential distributions, and the transition rates remain constant, satisfying the memoryless property. In contrast, semi-Markov switching allows more general sojourn-time distributions, such as Weibull distributions, with transition rates depending on the elapsed sojourn time. Therefore, Markov switching can be regarded as a special case of semi-Markov switching. Furthermore, considering the differences in dynamics and communication environments among heterogeneous agents, inconsistent semi-Markov switching–including $\sigma_1(t)$ and $\sigma_2(t)$–is adopted in this paper to characterize the distinct sojourn-time distributions and transition behaviors of first-order and second-order agents, allowing them to have different sojourn-time distributions and transition laws. Their joint modes determine the global communication topology, thereby incorporating the heterogeneous switching characteristics into the system model.*

Based on the inconsistent semi-Markov process, the global communication topology is determined by $\sigma_1(t)$ and $\sigma_2(t)$. Specifically, the adjacency matrix is represented as $A_{r(t)} = A_{\sigma_1(t),\sigma_2(t)}$. For any joint switching mode $(i, h) \in \mathcal{S}_1 \times \mathcal{S}_2$, the global adjacency matrix is defined as

$$A_{i,h} = \begin{bmatrix} A_{11}^{(i)} & A_{12}^{(i)} \\ A_{21}^{(h)} & A_{22}^{(h)} \end{bmatrix}, \tag{2.2}$$

where $A_{11}^{(i)}$ characterizes the communication relationships among first-order agents, $A_{12}^{(i)}$ characterizes the communication links through which first-order agents receive information from second-order agents, $A_{21}^{(h)}$ characterizes the communication links through which second-order agents receive information from first-order agents, and $A_{22}^{(h)}$ characterizes the communication relationships among second-order agents.

As shown in (2.2), the neighborhood sets of agents vary according to their respective switching modes. Specifically, the communication relationships associated with the first-order agents, including both intra-group and inter-group interactions, are governed by $A_{11}^{(\sigma_1(t))}$ and $A_{12}^{(\sigma_1(t))}$, respectively, whereas those associated with the second-order agents are determined by $A_{21}^{(\sigma_2(t))}$ and $A_{22}^{(\sigma_2(t))}$. Consequently, for each joint switching mode $(i, h) \in S_1 \times S_2$, the global communication topology is jointly determined by the simultaneous configurations $\sigma_1(t) = i$ and $\sigma_2(t) = h$. Accordingly, the corresponding global adjacency matrix and Laplacian matrix are denoted by $A^{i,h}$ and $L^{i,h}$, respectively. Therefore, a switching event in either semi-Markov process may alter the corresponding communication relationships and, consequently, the overall communication topology of the heterogeneous multi-agent system.

The corresponding degree matrix is defined as

$$D_{i,h} = \operatorname{diag}\left\{\sum_{j=1}^{n} a_{1j}^{(i,h)}, \ldots, \sum_{j=1}^{n} a_{nj}^{(i,h)}\right\},$$

where $a_{kj}^{(i,h)}$ denotes the (k, j)-th entry of the adjacency matrix $A_{i,h}$. Accordingly, the Laplacian matrix is given by $L_{r(t)} = D_{r(t)} - A_{r(t)}$, where $r(t) = (\sigma_1(t), \sigma_2(t)) = (i, h)$.

Remark 2. *The directed spanning tree condition is imposed on each admissible joint switching topology to guarantee sufficient information flow among all agents under every switching mode. This condition ensures that the corresponding Laplacian matrix has a simple zero eigenvalue and that the remaining eigenvalues have positive real parts. Such spectral properties provide the algebraic foundation for constructing the reduced consensus error system and analyzing its stability. In particular, they ensure that the relative-state representation can characterize the consensus objective without introducing additional connectivity conditions on the switching sequence. Therefore, the directed spanning tree condition is adopted to facilitate the consensus analysis under inconsistent semi-Markov switching topologies.*

In this paper, the considered composite attacks consist of additive deception attacks targeting the sensor measurement and actuator control channels of the HMASs. Specifically, malicious signals are injected into the sensor measurements to corrupt the state information available to the controller, while additional attack signals are injected into the actuator channels to manipulate the actual control inputs. These two types of attacks may occur simultaneously, resulting in corrupted state measurements and distorted control actions. Furthermore, the communication network topology is assumed to remain secure during the attack process. Based on this, attacks on actuators and sensors are modeled as follows:

$$\begin{aligned} x_i^c &= x_i + x_i^a, \\ v_i^c &= v_i + v_i^a, \end{aligned} \tag{2.3}$$

where x_i and v_i represent the true positions and velocities in the system, respectively. x_i^a and v_i^a are the attack signals, while x_i^c and v_i^c are corrupted state values that can be measured, transmitted to neighboring agents, and used in the controller.

Similarly, actuator attacks can be modeled as

$$u_i^c = u_i + u_i^a, \tag{2.4}$$

where u_i^a is the attack signal acting on the actuator and u_i^c is the control input value affected by the attack.

Assumption 2. *The attack signals $x_i^a(t)$, $v_i^a(t)$, and $u_i^a(t)$ are assumed to be continuously differentiable and bounded over the considered time interval. Their time derivatives are also bounded. These signals are deterministic and are not assumed to follow any specific probability distribution.*

For HMASs (2.1), the distributed control inputs u_i for each agent are

$$u_i = \begin{cases} -K_1 \left[\sum\limits_{j \in \mathcal{N}_i} a_{ij}(x_i^c - x_j^c) \right], i \in N_1, \\ -K_2 \left[\sum\limits_{j \in \mathcal{N}_i} a_{ij}(x_i^c - x_j^c) \right] - K_3 \left[\sum\limits_{j \in \mathcal{N}_{1i}} a_{ij}(v_i^c - v_j^c) \right], i \in N_2. \end{cases} \tag{2.5}$$

In (2.4), u_i^a represents the additive actuator deception signal, whereas (2.5) defines the nominal distributed consensus control protocol based on the corrupted sensor measurements. Therefore, the attack signals are explicitly characterized by x_i^a, v_i^a, and u_i^a, rather than by the control protocol itself.

According to the sensor attacks (2.3), actuator attacks (2.4), and control protocol attacks (2.5) described above, the HMASs (2.1) can be transformed into

$$\begin{cases} \begin{cases} \dot{x}_i = u_i + f_{1i}, \\ y_i = x_i^c, \end{cases} & i \in N_1, \\ \begin{cases} \dot{x}_i = v_i, \\ \dot{v}_i = u_i + f_{2i}, \\ y_{xi} = x_i^c, \\ y_{vi} = v_i^c, \end{cases} & i \in N_2, \end{cases} \tag{2.6}$$

where u_i is designed in (2.5). f_{1i} and f_{2i} are the total input signals received from sensors and actuators, described as

$$f_{1i} = -K_1 \sum a_{ij}(x_i^a - x_j^a) + u_i^a,$$

$$f_{2i} = -K_2 \sum a_{ij}(x_i^a - x_j^a) - K_3 \sum a_{ij}(v_i^a - v_j^a) + u_i^a.$$

To mitigate the effects of attacks on system performance while achieving secure consensus and reducing unnecessary communication resource consumption, a resilient control protocol is designed based on a dual ABETM. The overall design framework is illustrated in Figure 1. Specifically, to reduce redundant data transmission over the sensor-to-control and predictor-to-controller communication channels, two ABETMs, denoted as ABETM-a and ABETM-b, are respectively constructed. Additionally, to avoid the Zeno phenomenon, the designed ABETMs rely on sampled-data.

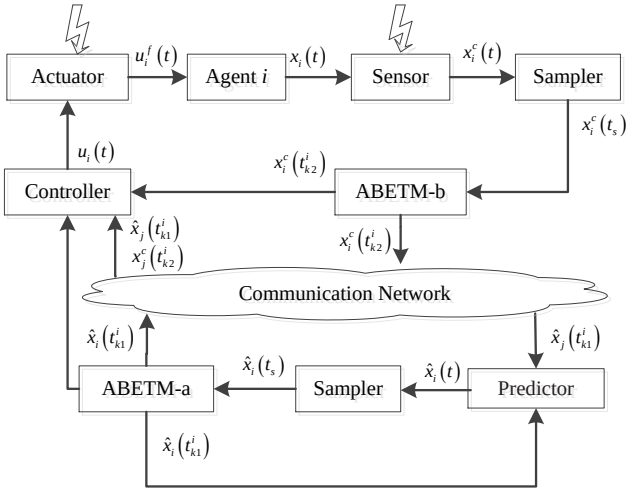

Figure 1. Framework for the overall design scheme.

First, to obtain the normal state of the system, a distributed state predictor is designed for each agent to estimate its expected normal state without attacks. The distributed state predictor is modeled as:

$$\begin{cases} \dot{\hat{x}}_i = u_{0i}, & i \in N_1, \\ \begin{cases} \dot{\hat{x}}_i = \hat{v}_i, \\ \dot{\hat{v}}_i = u_{0i}, \end{cases} & i \in N_2, \end{cases} \tag{2.7}$$

where $\hat{x}_i$ and $\hat{v}_i$ represent the predicted states of position and velocity for agent i. u_{0i} is designed as

$$u_{0i}(t) = \begin{cases} -K_1\left[\sum\limits_{j\in N_i} a_{ij}(\hat{x}_i(t_k^i) - \hat{x}_j(t_k^j))\right], i \in N_1, \\ -K_2\left[\sum\limits_{j\in N_i} a_{ij}(\hat{x}_i(t_k^i) - \hat{x}_j(t_k^j))\right] - K_3\left[\sum\limits_{j\in N_1} a_{ij}\left(\hat{v}_i(t_k^i) - \hat{v}_j(t_k^j)\right)\right], i \in N_2, \end{cases} \tag{2.8}$$

where t_k^i denotes the triggering instant of ABETM-a. The trigger conditions for ABETM-a from the predictor to the controller are designed as follows:

$$\begin{aligned} t_{k_1+1}^i &= \inf\{t_s > t_{k1}^i : E_{\hat{x}i}^{\mathrm{T}}(t_s)\Omega_1 E_{xi}(t_s) + \kappa\delta_{\hat{x}i}^{\mathrm{T}}(t_s)\Omega_1\delta_{xi}(t_s) - \sigma_1\hat{X}^{\mathrm{T}}(t_s)\Omega_1\hat{X}(t_s) \geq 0\}, i \in N_1, \\ t_{k_1+1}^i &= \inf\{t_s > t_{k1}^i : E_{\hat{x}i}^{\mathrm{T}}(t_s)\Omega_2 E_{xi}(t_s) + \kappa\delta_{\hat{x}i}^{\mathrm{T}}(t_s)\Omega_2\delta_{xi}(t_s) - \sigma_1\hat{X}^{\mathrm{T}}(t_s)\Omega_2\hat{X}(t_s) \geq 0\}, i \in N_2, \\ t_{k_1+1}^i &= \inf\{t_s > t_{k1}^i : E_{\hat{v}i}^{\mathrm{T}}(t_s)\Omega_3 E_{vi}(t_s) + \kappa\delta_{\hat{v}i}^{\mathrm{T}}(t_s)\Omega_3\delta_{vi}(t_s) - \sigma_1\hat{V}^{\mathrm{T}}(t_s)\Omega_3\hat{V}(t_s) \geq 0\}, i \in N_2, \end{aligned} \tag{2.9}$$

where

$$\mathcal{E}_{\hat{x}i}(t_s) = \int_{t_k^i}^{t_s} \delta_{\hat{x}_i}(s)ds, \mathcal{E}_{vi}(t_s) = \int_{t_k^i}^{t_s} \delta_{\hat{v}_i}(s)ds$$

represent the accumulated state error over the interval from the most recent triggering instant t_k^i to the current sampling instant t_s, respectively. $\delta_{\hat{x}_i}(s) = \hat{x}_i(s) - \hat{x}_i(t_k^i)$ and $\delta_{\hat{v}_i}(s) = \hat{v}_i(s) - \hat{v}_i(t_k^i)$ denote the deviation of the predicted position and velocity of agent i at time s from their respective values at the most recent triggering instant t_k^i. t_s denotes the sampling time, which satisfies $0 = t_0 < t_1 < ... < t_s < ....$ $\sigma_\alpha > 0$ denotes the threshold parameter and Ω_α is the adjustment parameter matrix to be designed, $\alpha = 1, 2, 3$. Define compact variables

$$\mathcal{E}_{ai} = \mathrm{col}\{\mathcal{E}_{\mathrm{xi}}, \mathcal{E}_{\mathrm{xj}}, \mathcal{E}_{\mathrm{vj}}\},\ \delta_{\mathrm{ai}} = \mathrm{col}\{\delta_{\hat{\mathrm{x}}_\mathrm{i}}, \delta_{\hat{\mathrm{x}}_\mathrm{j}}, \delta_{\hat{\mathrm{v}}_\mathrm{j}}\},$$

where $i \in N_1$, $j \in N_2$, $\sigma_a = \mathrm{diag}\{\sigma_1, \sigma_2, \sigma_3\}$, $\Omega_a = \mathrm{diag}\{\Omega_1, \Omega_2, \Omega_3\}$. Then, the trigger conditions (2.9) can be represented as

$$t_{k1+1}^i = \inf\{t_s > t_k^i : \mathcal{E}_{ai}^{\mathrm{T}}(t_s)\Omega_a\mathcal{E}_{ai}(t_s) + \kappa\delta_{\hat{a}i}^{\mathrm{T}}(t_s)\Omega_a\delta_{ai}(t_s) - \sigma_a e_c^{\mathrm{T}}(t_s)\Omega_a e_c(t_s) \geq 0\}. \tag{2.10}$$

Remark 3. *The proposed ABETM differs from conventional event-triggered mechanisms based on instantaneous errors. Instead of evaluating the state deviation only at the current sampling instant, the proposed mechanism considers its accumulation over the interval between two consecutive triggering instants. This design provides a temporal measure of the prediction error and reduces the sensitivity of triggering decisions to isolated instantaneous fluctuations. From an engineering perspective, it helps avoid unnecessary data transmissions and control updates in networked heterogeneous multi-agent systems, thereby improving communication resource utilization while maintaining the required control performance. Moreover, the state-dependent threshold allows the triggering decision to be adjusted according to the current state magnitude.*

To mitigate the impact of attacks on HMASs, the following distributed resilient control protocol is proposed:

$$u_i = u_{1i} + u_{2i}, \tag{2.11}$$

where u_{1i} is responsible for maintaining the robustness of the system, while u_{2i} is responsible for defending against attacks on actuators and preventing sensor attacks from compromised agents from spreading to other agents.

Based on the above design of the resilient controller (2.11), HMASs (2.1) under actuator/sensor attacks can be characterized as follows:

$$\begin{cases} \dot{x}_i = u_{1i} + u_{2i} + f_{1i}, i \in N_1, \\ \begin{cases} \dot{x}_i = v_i, \\ \dot{v}_i = u_{1i} + u_{2i} + f_{2i} \end{cases}, i \in N_2, \end{cases} \tag{2.12}$$

where the controller is designed as follows:

$$u_{1i} = \begin{cases} -K_1 \left[\sum\limits_{j \in N(i)} a_{ij} (\hat{x}_i(t^i_{k2}) - \hat{x}_j(t^i_{k2})) \right], i \in N_1, \\ -K_2 \left[\sum\limits_{j \in N(i)} a_{ij} \left(\hat{x}_i(t^i_{k2}) - \hat{x}_j(t^i_{k2}) \right) \right] - K_3 \left[\sum\limits_{j \in N_1(i)} a_{ij} \left(\hat{v}_i(t^i_{k2}) - \hat{v}_j(t^i_{k2}) \right) \right], i \in N_2, \end{cases} \tag{2.13}$$

$$u_{2i} = \begin{cases} -K^x_1 \left[\sum\limits_{j \in N(i)} a_{ij} \left(\bar{x}_i(t^i_{k2}) - \bar{x}_j(t^i_k) \right) - \sum\limits_{j \in N(i)} a_{ij} \left(\hat{x}_i(t^i_{k2}) - \hat{x}_j(t^i_{k2}) \right) \right] - \hat{f}_i, i \in N_1, \\ -K^x_2 \left[\sum\limits_{j \in N(i)} a_{ij} \left(\bar{x}_i(t^i_{k2}) - \bar{x}_j(t^i_{k2}) \right) - \sum\limits_{j \in N(i)} a_{ij} \left(\hat{x}_i(t^i_{k2}) - \hat{x}_j(t^i_{k2}) \right) \right] \\ -K^x_3 \left[\sum\limits_{j \in N_1(i)} a_{ij} \left(\bar{v}_i(t^i_{k2}) - \bar{v}_j(t^i_{k2}) \right) - \sum\limits_{j \in N_1(i)} a_{ij} \left(\hat{v}_i(t^i_{k2}) - \hat{v}_j(t^i_{k2}) \right) \right] - \hat{f}_i, i \in N_2, \end{cases} \tag{2.14}$$

with

$$\dot{\hat{f}}_i = \begin{cases} K^f_1 \left(\bar{x}_i(t^i_{k2}) - \hat{x}_i(t^i_{k2}) \right) - \hat{f}_i, i \in N_1, \\ K^f_2 \left(\bar{x}_i(t^i_{k2}) - \hat{x}_i(t^i_{k2}) \right) + K^f_3 \left(v_i(t^i_{k2}) - \hat{v}_i(t^i_{k2}) \right) - \hat{f}_i, i \in N_2, \end{cases} \tag{2.15}$$

where $\hat{f}_i$ is the estimate of the attack. t^i_{k2} is the most recent triggering instant of the ABETM-b from the sensor to the controller. The triggering condition is

$$\begin{aligned} t^i_{k2+1} &= \inf\{t_s > t^i_{k2} : \mathcal{E}^{c\mathrm{T}}_{xi}(t_s)\Omega_4\mathcal{E}^c_{xi}(t_s) + \kappa\delta^{\mathrm{T}}_{xi}(t_s)\Omega_4\delta_{xi}(t_s) - \sigma_4 e^{\mathrm{T}}_{xi}(t_s)\Omega_4 e_{xi}(t_s) \geq 0\}, i \in N_1, \\ t^i_{k2+1} &= \inf\{t_s > t^i_{k2} : \mathcal{E}^{c\mathrm{T}}_{xi}(t_s)\Omega_5\mathcal{E}^c_{xi}(t_s) + \kappa\delta^{\mathrm{T}}_{xi}(t_s)\Omega_5\delta_{xi}(t_s) - \sigma_5 e^{\mathrm{T}}_{xi}(t_s)\Omega_5 e_{xi}(t_s) \geq 0\}, i \in N_2, \\ t^i_{k2+1} &= \inf\{t_s > t^i_{k2} : \mathcal{E}^{c\mathrm{T}}_{vi}(t_s)\Omega_6\mathcal{E}^c_{vi}(t_s) + \kappa\delta^{\mathrm{T}}_{vi}(t_s)\Omega_6\delta_{vi}(t_s) - \sigma_5 e^{\mathrm{T}}_{vi}(t_s)\Omega_6 e_{vi}(t_s) \geq 0\}, i \in N_2, \end{aligned} \tag{2.16}$$

where $\mathcal{E}^c_{xi}(t_s) = \int^{t_s}_{t^i_{k2}} \delta_{x_i}(s)ds$, $\mathcal{E}^c_{vi}(t_s) = \int^{t_s}_{t^i_{k2}} \delta_{v_i}(s)d\tau$ represent the accumulated position and velocity measurement errors over the interval from the most recent triggering instant t^i_{k2} to the current sampling instant t_s, respectively. $\delta_{x_i}(t_s) = x^c_i(t_s) - x^c_i(t^i_{k2})$, $\delta_{v_i}(t_s) = v^c_i(t_s) - v^c_i(t^i_{k2})$ denote the deviations of the measured position and velocity of agent i at time t_s from their respective values at the most recent triggering instant t^i_{k2}. $\sigma_\alpha > 0$ denotes the threshold parameter and Ω_α is adjustment parameter matrix to be designed, with $\alpha = 4, 5, 6$. Define compact variables $\mathcal{E}_{bi} = \mathrm{col}\{\mathcal{E}^{\mathrm{c}}_{\mathrm{xi}}, \mathcal{E}^{\mathrm{c}}_{\mathrm{xj}}, \mathcal{E}^{\mathrm{c}}_{\mathrm{vj}}\}$, $\delta_{bi} = \mathrm{col}\{\delta_{\mathrm{x_i}}, \delta_{\mathrm{x_j}}, \delta_{\mathrm{v_j}}\}$, where $i \in N_1$, $j \in N_2$. $\sigma_b = \mathrm{diag}\{\sigma_4, \sigma_5, \sigma_6\}$, $\Omega_b = \mathrm{diag}\{\Omega_4, \Omega_5, \Omega_6\}$. Then, triggering conditions (2.9) can be represented as

$$t^i_{k2+1} = \inf\{t_s > t^i_k : \mathcal{E}^T_{bi}(t_s)\Omega_b\mathcal{E}_{bi}(t_s) + \kappa\delta^{\mathrm{T}}_{bi}(t_s)\Omega_b\delta_{bi}(t_s) - \sigma_b e^{\mathrm{T}}_i(t_s)\Omega_b e_i(t_s) \geq 0\}. \tag{2.17}$$

To facilitate the stability analysis, we define the sampling-induced time-varying delay as $0 \leq \eta(t) = t - t_s \leq \eta_M, \dot{\chi}(t) = 1$. We define the state error $e_{x_i} = x_i - \hat{x}_i$ and the attack estimation error as $\tilde{f}_i = f_i - \hat{f}_i$. When $i \in N_1$, the error system can be expressed as follows:

$$\dot{e}_{xi} = -(L \otimes K_i^x)e_{xi\eta} + (L \otimes K_i^x)\delta_{xi\eta} + \tilde{f}_i. \tag{2.18}$$

The attack error estimation system can be expressed as follows:

$$\dot{\tilde{f}}_{1i}(t) = \dot{f}_{1i} - \dot{\hat{f}}_i = -K_1^f e_{xi\eta} + K_1^f \delta_{xi\eta} - \tilde{f}_i + f_{1i} + \dot{f}_{1i}. \tag{2.19}$$

Similarly, when $i \in N_2$, the error system is expressed as follows:

$$\begin{cases} \dot{e}_{xi} = e_{vi}, \\ \dot{e}_{vi} = -(L \otimes K_2^x)e_{xi\eta} + (L \otimes K_2^x)\delta_{xi\eta} - (L \otimes K_3^x)e_{xi\eta} + (L \otimes K_3^x)\delta_{xi\eta} + \tilde{f}_i. \end{cases} \tag{2.20}$$

The attack error estimation system is as follows:

$$\dot{\tilde{f}}_{2i}(t) = -K_2^f e_{xi\eta} + K_2^f \delta_{xi\eta} - K_3^f e_{vi\eta} + K_3^f \delta_{vi\eta} - \tilde{f}_i + \dot{f}_{2i} + f_{2i}. \tag{2.21}$$

Combining the above equations yields the following compact form of the global error system:

$$\dot{\tilde{e}}_i = \begin{bmatrix} \tilde{A} \\ 0 \end{bmatrix} e + \begin{bmatrix} \tilde{B}_1 \\ -\tilde{I} \end{bmatrix} \tilde{f}_i - \begin{bmatrix} L \otimes \tilde{K}_x \\ \tilde{K}_f \end{bmatrix} \tilde{e}_{i\eta} + \begin{bmatrix} L \otimes \tilde{K}_x \\ \tilde{K}_f \end{bmatrix} \delta_{i\eta} + \begin{bmatrix} 0 \\ \tilde{C} \end{bmatrix} \tilde{F}, \tag{2.22}$$

where $\tilde{e}_i = \text{col}[e_i, \tilde{f}_i]$, with $e_i = \text{col}[e_{x_i}, e_{x_j}, e_{v_j}]$, $\tilde{f}_i = \text{col}[\tilde{f}_{1i}, \tilde{f}_{2i}]$. e_i and $\tilde{f}_i$ represent the global state error and global attack error of the system, respectively. The parameters of the correlation matrix in the error system (2.22) are expressed as follows:

$$\tilde{A} = \begin{bmatrix} 0 & 0 & 0 \\ 0 & 0 & \mathscr{I}_2 \\ 0 & 0 & 0 \end{bmatrix}, \tilde{B}_1 = \begin{bmatrix} \mathscr{I}_1 & 0 \\ 0 & 0 \\ 0 & \mathscr{I}_2 \end{bmatrix}, \tilde{I} = \begin{bmatrix} \mathscr{I}_1 & 0 \\ 0 & \mathscr{I}_2 \end{bmatrix}, \tilde{K}_x = \begin{bmatrix} K_1^x & 0 & 0 \\ 0 & 0 & K_2^x \\ 0 & 0 & K_3^x \end{bmatrix},$$
$$\tilde{K}_f = \begin{bmatrix} K_1^f & 0 & 0 \\ 0 & K_2^f & K_3^f \end{bmatrix}, \tilde{C} = \begin{bmatrix} \mathscr{I}_1 & 0 & \mathscr{I}_1 & 0 \\ 0 & \mathscr{I}_2 & 0 & \mathscr{I}_2 \end{bmatrix}, \tilde{F} = \text{col}\{f_{1i}, f_{2i}, \dot{f}_{1i}, \dot{f}_{2i}\},$$

with $\mathscr{I}_1 = \mathscr{I}_m$, $\mathscr{I}_2 = \mathscr{I}_{n-m}$.

The above steps analyze the state estimation problem for HMASs subject to attacks under inconsistent semi-Markov switching topologies, which provide reliable state information for subsequent consensus analysis. By designing resilient controller (2.11), attack estimator (2.15), and event-triggered mechanism (2.9), (2.16), thereby ensuring the stability of the error system (2.22) under the following condition: for non-zero $\tilde{F}$, $\|\tilde{e}_i\|_2 \leq \beta \left\|\tilde{F}_i\right\|_2$.

Next, the consensus problem of the system is further analyzed. Before analyzing consensus, some necessary algebraic operations need to be performed. To characterize the consensus behavior of all agents, we define $\hat{X}(t) = \text{col}\{\hat{x}_1(t), \ldots, \hat{x}_n(t)\}$, $\hat{V}(t) = \text{col}\{\hat{v}_{m+1}(t), \ldots, \hat{v}_n(t)\}$. Let $C_n = [-\mathbf{1}_{n-1}, I_{n-1}]$ and the global position errors are defined as $\bar{X}(t) = (C_n \otimes I_p)\hat{X}(t)$. Thus, the global consensus error is given by $e_c(t) = \text{col}\{\bar{X}(t), \hat{V}(t)\}$.

Accordingly, based on the predictor dynamics and the control protocol, the global consensus error system under the joint switching mode $r = (i, h)$ can be expressed as

$$\dot{e}_c = A_0 e_c + (A_r \otimes K)e_{c\eta} + (B_r \otimes K)\delta_{c\eta}, \tag{2.23}$$

where

$$A_0 = \begin{bmatrix} 0 & (C_n S_2) \otimes I_p \\ 0 & 0 \end{bmatrix}, A_r = \begin{bmatrix} -(C_n \Pi_1 L_r D_n) \otimes I_p & 0 \\ -(S_2^T L_r D_n) \otimes I_p & -L_{\mathrm{v}}^{(h)} \otimes I_p \end{bmatrix},$$
$$B_r = \begin{bmatrix} (C_n \Pi_1 L_r) \otimes I_p & 0 \\ (S_2^T L_r) \otimes I_p & L_{\mathrm{v}}^{(h)} \otimes I_p \end{bmatrix}, \Pi_1 = S_1 S_1^T, D_n = \begin{bmatrix} 0_{1\times(n-1)} \\ I_{n-1} \end{bmatrix}, S_1 = \begin{bmatrix} I_m \\ 0 \end{bmatrix}, S_2 = \begin{bmatrix} 0 \\ I_{n-m} \end{bmatrix}.$$

Based on the stability of the prediction error system, the consensus error system is constructed by utilizing state information obtained from the state predictor. The stability of the system was ensured with the designed controller and ABETM.

3. Main results

In this section, two theorems are presented to establish sufficient conditions for resilient consensus of the considered HMASs. Specifically, Theorem 1 addresses the stability of the augmented error system involving state and attack estimation errors, whereas Theorem 2 focuses on the stability of the consensus error system. Together, they provide theoretical guarantees for resilient consensus under composite attacks.

Theorem 1. *Under Assumption 1, each admissible joint switching topology $\mathcal{G}^{i,h}$, $(i, h) \in S_1 \times S_2$, contains a directed spanning tree. Given scalars λ, κ, β_1, ϑ_1, τ_M, σ_4, σ_5, and σ_6, the error system (2.22) is finite-L_2-gain stable if there exist positive-definite matrices $\mathcal{P}$, $\tilde{Q}_1$, $\tilde{Q}_2$ and matrices $\tilde{Z}_1$, $\tilde{Z}_2$, $\tilde{\Omega}$ of appropriate dimensions such that:*

$$\Gamma = \begin{bmatrix} \Gamma_{11} & \Gamma_{12} & \Gamma_{13} & \Gamma_{14} & \Gamma_{15} & 0 & \Gamma_{17} & \Gamma_{18} & 0 & \Gamma_{1,10} \\ * & \Gamma_{22} & \Gamma_{23} & \Gamma_{24} & \Gamma_{25} & 0 & \Gamma_{27} & \Gamma_{28} & \Gamma_{29} & 0 \\ * & * & \Gamma_{33} & \Gamma_{34} & \Gamma_{35} & 0 & 0 & \Gamma_{38} & \Gamma_{39} & 0 \\ * & * & * & \Gamma_{44} & 0 & 0 & 0 & 0 & 0 & 0 \\ * & * & * & * & \Gamma_{55} & 0 & \Gamma_{57} & \Gamma_{58} & \Gamma_{59} & 0 \\ * & * & * & * & * & \Gamma_{66} & 0 & 0 & 0 & 0 \\ * & * & * & * & * & * & \Gamma_{77} & 0 & \Gamma_{79} & 0 \\ * & * & * & * & * & * & * & \Gamma_{88} & 0 & 0 \\ * & * & * & * & * & * & * & * & \Gamma_{99} & 0 \\ * & * & * & * & * & * & * & * & * & \Gamma_{10,10} \end{bmatrix} < 0, \tag{3.1}$$

where

$$\Gamma_{11} = \mathscr{I}_3 \otimes \mathcal{J}_{i,h}(\mathcal{P}) + 2\tilde{A} \otimes \mathcal{P} + \mathscr{I}_3 \otimes \tilde{Q}_1 - \mathscr{I}_3 \otimes \tilde{Z}_1, \mathscr{I}_3 = \mathrm{diag}\{\mathscr{I}_1, \mathscr{I}_2, \mathscr{I}_2\},$$
$$\Gamma_{12} = \tilde{B}_1 \otimes \mathcal{P}, \Gamma_{13} = -L \otimes Y_1 + \mathscr{I}_3 \otimes \tilde{Z}_1 - \mathscr{I}_3 \otimes \tilde{Z}_2, \Gamma_{14} = \mathscr{I}_3 \otimes \tilde{Z}_2, \Gamma_{15} = L \otimes Y_1,$$
$$\Gamma_{22} = \mathscr{I}_4 \otimes (2\mathcal{P} + \tilde{Q}_1 - \tilde{Z}_1), \mathscr{I}_4 = \mathrm{diag}\{\mathscr{I}_1, \mathscr{I}_2\}, \Gamma_{23} = \mathscr{I}_4 \otimes (-Y_2 + \tilde{Z}_1 - \tilde{Z}_2),$$
$$\Gamma_{24} = \mathscr{I}_4 \otimes \tilde{Z}_2, \Gamma_{25} = \mathscr{I}_4 \otimes Y_2, \Gamma_{26} = \mathscr{I}_4 \otimes \tilde{C}_f, \Gamma_{33} = \mathscr{I}_5 \otimes (-2\tilde{Z}_1 + \tilde{Z}_2 + \tilde{Z}_2^{\mathrm{T}} + \lambda\Phi_1),$$

$$\mathscr{I}_5 = \text{diag}\{\mathscr{I}_3, \mathscr{I}_4\}, \Phi_1 = \text{diag}\{\sigma_4\tilde{\Omega}_4, \sigma_5\tilde{\Omega}_5, \sigma_6\tilde{\Omega}_6, 0, 0\}, \Gamma_{34} = \mathscr{I}_5 \otimes (\tilde{Z}_1 - \tilde{Z}_2),$$
$$\Gamma_{35} = \mathscr{I}_5 \otimes \Phi_2, \Phi_2 = \text{diag}\{\Omega_4, \Omega_5, \Omega_6; 0_{2\times 3}), \Gamma_{44} = -\mathscr{I}_5 \otimes (\tilde{Q}_1 + \tilde{Z}_1), \Gamma_{55} = -\mathscr{I}_3 \otimes \lambda\kappa\Omega_b,$$
$$\Gamma_{66} = -\mathscr{I}_3 \otimes \lambda\Omega_b, \Gamma_{77} = -\beta^2 \otimes \mathscr{I}_4, \Gamma_{18} = \tilde{A}^{\mathrm{T}} \otimes \mathcal{P}, \Gamma_{28} = \tilde{B}^{\mathrm{T}} \otimes \mathcal{P}, \Gamma_{38} = -[L \otimes Y_1; 0],$$
$$\Gamma_{58} = [L \otimes Y_1; 0], \Gamma_{29} = \mathscr{I}_4 \otimes \mathcal{P}, \Gamma_{39} = -[\mathscr{I}_4 \otimes Y_2; 0], \Gamma_{59} = [\mathscr{I}_4 \otimes Y_2; 0], \Gamma_{79} = \tilde{C} \otimes \mathcal{P},$$
$$\Gamma_{88} = \mathscr{I}_3 \otimes (\vartheta_1^2\tau_M^2\tilde{Q}_2 - 2\vartheta_1\mathcal{P}), \Gamma_{99} = \mathscr{I}_4 \otimes (\vartheta_1^2\tau_M^2\tilde{Q}_2 - 2\vartheta_1\mathcal{P}), \Gamma_{1,10} = \mathscr{I}_3, \Gamma_{10,10} = -\mathscr{I}_3,$$

meeting the predefined conditions. In addition, the parameter matrix can be obtained: $\tilde{K} = Y_1\mathcal{P}^{-1}$.

Proof. Construct the Lyapunov function as

$$V_1(t,\sigma) = e^{\mathrm{T}}P_\sigma e + \tilde{f}^{\mathrm{T}}P_\sigma\tilde{f} + \int_{t-\tau_M}^{t} \tilde{e}^T(s)\,Q_1\tilde{e}(s)\,ds + \tau_M \int_{-\tau_M}^{0}\int_{t+\theta}^{t} \dot{\tilde{e}}^T(s)\,Q_2\dot{\tilde{e}}(s)\,ds d\theta. \tag{3.2}$$

When $\sigma(t) = m$, by applying the weak infinitesimal operator $\mathcal{L}$ in [35], we have

$$\begin{aligned} LV_1(t,\sigma(t)) = {} & 2e^{\mathrm{T}}P_m\left(\tilde{A}e_i + \tilde{B}_1\tilde{f}_i - L\otimes\tilde{K}_x\tilde{e}_{i\eta} + L\otimes\tilde{K}_x\tilde{\delta}_{i\eta}\right) + e^{\mathrm{T}}\mathcal{J}_{i,h}(P)e \\ & + 2\tilde{f}^{\mathrm{T}}P_l\left(\tilde{f} - \tilde{K}_f\tilde{e}_{i\eta} + \tilde{K}_f\tilde{\delta}_{i\eta} + \tilde{C}\tilde{F}\right) + \tilde{e}^TQ_1\tilde{e} - \tilde{e}^T(t-\tau_M)\,Q_1\tilde{e}(t-\tau_M) \\ & + \tau_M^2\dot{\tilde{e}}^TQ_2\dot{\tilde{e}} - \tau_M\int_{t-\tau_M}^{t}\dot{\tilde{e}}^T(s)\,Q_2\dot{\tilde{e}}(s)\,ds, \end{aligned} \tag{3.3}$$

where $\mathcal{J}_{i,h}(P) = \sum_{(j,k)\neq(i,h)} q_{(i,h),(j,k)}(P_{j,k} - P_{i,h})$.

Furthermore, according to [36], one yields

$$-\tau_M\int_{t-\tau_M}^{t}\dot{\tilde{e}}^T(s)\,Q_2\tilde{e}(s)\,ds \le \theta_0^{\mathrm{T}}\Theta_0\theta_0, \tag{3.4}$$

where

$$\theta_0 = \text{col}\left[\tilde{e}, \tilde{e}(t-\eta(t)), \tilde{e}(t-\tau_M)\right],$$
$$\Theta_0 = \begin{bmatrix} -Z_1 & Z_1 - Z_2 & Z_2 \\ * & -2Z_1 + Z_2 + Z_2^{\mathrm{T}} & Z_1 - Z_2 \\ * & * & -Z_1 \end{bmatrix}.$$

Based on the trigger condition (2.17), and the S-procedure lemma [37], one derives

$$\lambda(\sigma_b e_i^{\mathrm{T}}(t_s)\Omega_b e_i(t_s) - \mathcal{E}_{bi}^T(t_s)\Omega_b\mathcal{E}_{bi}(t_s) - \kappa\delta_{bi}^{\mathrm{T}}(t_s)\Omega_b\delta_{bi}(t_s)) \ge 0. \tag{3.5}$$

By combining the above expressions, ABETM-b, and the Kronecker product, and defining $\theta_1 = \text{col}\left[e, \tilde{f}, \tilde{e}_\tau, \tilde{e}(t-\tau_M), \tilde{\delta}_\tau, \mathcal{E}_{bi}, \tilde{F},\right]$, it follows that

$$\begin{aligned} \mathrm{E}\{LV(t,\sigma(t))\} &\le \theta_1^{\mathrm{T}}\Theta_1\theta_1 + \tau_M^2\dot{\tilde{e}}^{\mathrm{T}}Q_2\dot{\tilde{e}} - \tilde{e}^{\mathrm{T}}\tilde{e} + \beta^2\tilde{F}^{\mathrm{T}}\tilde{F} \\ &\le \theta_1^{\mathrm{T}}\left(\Theta_1 + \Theta_2^{\mathrm{T}}\left(\tau_M^2Q_2\right)\Theta_2\right)\theta_1 - \tilde{e}^{\mathrm{T}}\tilde{e} + \beta^2\tilde{F}^{\mathrm{T}}\tilde{F}. \end{aligned}$$

Then, by applying the Schur complement lemma [38], one obtains Θ as:

$$\Theta = \begin{bmatrix} \Theta_1 & \Theta_{12}^{\mathrm{T}} & \Theta_{13} \\ * & \Theta_{22} & 0 \\ * & * & \Theta_{33} \end{bmatrix} \tag{3.6}$$

where

$$\Theta_1 = \begin{bmatrix} \Theta_{111} & \Theta_{112} & \Theta_{113} & \Theta_{114} & \Theta_{115} & 0 & 0 \\ * & \Theta_{122} & \Theta_{123} & \Theta_{124} & \Theta_{125} & 0 & \Theta_{127} \\ * & * & \Theta_{133} & \Theta_{134} & \Theta_{135} & 0 & 0 \\ * & * & * & \Theta_{144} & 0 & 0 & 0 \\ * & * & * & * & \Theta_{155} & 0 & 0 \\ * & * & * & * & * & \Theta_{166} & 0 \\ * & * & * & * & * & * & \Theta_{177} \end{bmatrix},$$
$$\Theta_{12} = \mathscr{I}_5 \otimes \begin{bmatrix} \tilde{A} & \tilde{B} & -L \otimes \tilde{B}_2\tilde{K}_x & 0 & L \otimes \tilde{B}_2\tilde{K}_x & 0 \\ 0 & \tilde{I} & -\tilde{K}_f & 0 & \tilde{K}_f & \tilde{C} \end{bmatrix},$$
$$\Theta_{22} = \mathscr{I}_5 \otimes \mathrm{diag}\left\{-\left(\tau_M^2 Q_2\right)^{-1}, -\left(\tau_M^2 Q_2\right)^{-1}\right\},$$
$$\Theta_{13} = \mathrm{col}[\mathscr{I}_3, 0, 0, 0, 0, 0], \Theta_{33} = -\mathscr{I}_3, \tag{3.7}$$

with

$$\Theta_{111} = 2P_l \otimes \tilde{A} + \mathscr{I}_3 \otimes (\mathcal{J}_{i,h}(P) + Q_1 - Z_1), \Theta_{112} = P_l \otimes \tilde{B}_1, \Theta_{114} = \mathscr{I}_3 \otimes Z_2,$$
$$\Theta_{113} = -P_l(L \otimes \tilde{K}_x) + \mathscr{I}_3 \otimes (Z_1 - Z_2), \Theta_{115} = P_l(L \otimes \tilde{K}_x), \Theta_{122} = \mathscr{I}_4 \otimes (2P_l + Q_1 - Z_1),$$
$$\Theta_{123} = -\mathscr{I}_4 \otimes (P_l\tilde{K}_f - Z_1 + Z_2), \Theta_{124} = \mathscr{I}_4 \otimes (Z_2), \Theta_{125} = \mathscr{I}_4 \otimes (P_l\tilde{K}_f), \Theta_{127} = \mathscr{I}_4 \otimes (P_l\tilde{C}_f),$$
$$\Theta_{133} = \mathscr{I}_5 \otimes (-2Z_1 + Z_2 + Z_2^{\mathrm{T}} + \Phi_1), \Theta_{134} = \mathscr{I}_5 \otimes (Z_1 - Z_2), \Theta_{135} = \mathscr{I}_5 \otimes \Phi_2,$$
$$\Theta_{144} = \mathscr{I}_5 \otimes (-Q_1 - Z_1), \Theta_{155} = -\mathscr{I}_3 \otimes \lambda\kappa\Omega_b, \Theta_{166} = -\mathscr{I}_3 \otimes \lambda\Omega_b, \Theta_{177} = -\beta^2 \otimes \mathscr{I}_4.$$

We define $\mathcal{P} = P_l^{-1}$, $\tilde{Q}_1 = \mathcal{P}^{\mathrm{T}}Q_1\mathcal{P}$, $\tilde{Q}_2 = \mathcal{P}^{\mathrm{T}}Q_2\mathcal{P}$, $\tilde{Z}_1 = \mathcal{P}^{\mathrm{T}}Z_1\mathcal{P}$, $\tilde{Z}_2 = \mathcal{P}^{\mathrm{T}}Z_2\mathcal{P}$, and $\tilde{\Omega} = \mathcal{P}^{\mathrm{T}}\Omega\mathcal{P}$. Then, pre- and post-multiplying both sides of (15) by diag $\{\mathcal{P}, \mathcal{P}, \mathcal{P}, \mathcal{P}, \mathcal{P}, I, I, I, I\}$ and its transpose, one has

$$\Gamma = \begin{bmatrix} \Gamma_{11} & \Gamma_{12} & \Gamma_{13} & \Gamma_{14} & \Gamma_{15} & 0 & \Gamma_{17} & \Gamma_{18} & 0 & \Gamma_{1,10} \\ * & \Gamma_{22} & \Gamma_{23} & \Gamma_{24} & \Gamma_{25} & 0 & \Gamma_{27} & \Gamma_{28} & \Gamma_{29} & 0 \\ * & * & \Gamma_{33} & \Gamma_{34} & \Gamma_{35} & 0 & 0 & \Gamma_{38} & \Gamma_{39} & 0 \\ * & * & * & \Gamma_{44} & 0 & 0 & 0 & 0 & 0 & 0 \\ * & * & * & * & \Gamma_{55} & 0 & \Gamma_{57} & \Gamma_{58} & \Gamma_{59} & 0 \\ * & * & * & * & * & \Gamma_{66} & 0 & 0 & 0 & 0 \\ * & * & * & * & * & * & \tilde{\Theta}_{77} & 0 & \Gamma_{79} & 0 \\ * & * & * & * & * & * & * & \tilde{\Theta}_{88} & 0 & 0 \\ * & * & * & * & * & * & * & * & \Gamma_{99} & 0 \\ * & * & * & * & * & * & * & * & * & \Gamma_{10,10} \end{bmatrix} < 0, \tag{3.8}$$

where the elements are defined as shown in (3.1). Moreover, from Lemma 3 in [39], one has the following:

$$\tilde{\Theta}_{77} = -I_5 \otimes \left(\tau_M^2 Q_2\right)^{-1} = -I_5 \otimes \mathcal{P}\left(\tau_M^2 \tilde{Q}_2\right)^{-1}\mathcal{P} \leq I_5 \otimes (\vartheta_1^2\tau_M^2\tilde{Q}_2 - 2\vartheta_1\mathcal{P}) = \Gamma_{77}. \tag{3.9}$$

Similarly, Γ_{88} is derived. Then, it can be obtained Γ as in (3.1). If the inequality in (3.1) holds, one derives $\mathrm{E}\{V(e(+\infty))\} - \mathrm{E}\{V(e(0))\} \leq \mathrm{E}\left\{\int_0^{+\infty}\left(-\tilde{e}^{\mathrm{T}}\tilde{e} + \beta^2\tilde{F}^{\mathrm{T}}\tilde{F}\right)dt\right\}$. Under zero initial condition $V(e(0)) = 0$, it is easy to find that $\mathrm{E}\{V(e(+\infty))\} = \mathrm{E}\left\{\int_0^{+\infty}\mathcal{L}V(t, \sigma(t))dt\right\} \geq 0$. Furthermore, one can get $\mathrm{E}\left\{\int_0^{+\infty}\tilde{e}^{\mathrm{T}}\tilde{e}dt\right\} \leq \beta^2\mathrm{E}\left\{\int_0^{+\infty}\tilde{F}^{\mathrm{T}}\tilde{F}dt\right\}$. Therefore, the estimation error system possesses a finite L_2-gain

with respect to the disturbance input. When the external disturbance satisfies $\tilde{F} \in L_2[0,\infty)$, it follows that $\tilde{e} \in L_2[0,\infty)$. Furthermore, under the boundedness conditions of the closed-loop error dynamics, the derivative of the augmented error state is bounded. Consequently, $\tilde{e}(t)$ is uniformly continuous. By applying Barbalat's lemma, one obtains $\lim_{t\to\infty} \tilde{e}(t) = 0$. This completes the proof. □

Theorem 2. *Under Assumption 1, each admissible joint switching topology $\mathcal{G}^{i,h}$, $(i,h) \in S_1 \times S_2$, contains a directed spanning tree. Given scalars β_2, ϑ_2, τ_M, σ_1, σ_2 and σ_3, if there exist positive-definite matrices $\bar{R}$, $\bar{Q}_3$, $\bar{Q}_4$ and appropriate-dimensions matrices $\bar{Z}_3$, $\bar{Z}_4$, $\bar{\Omega}$ such that:*

$$\Lambda = \begin{bmatrix} \Lambda_{11} & \Lambda_{12} & \Lambda_{13} & \Lambda_{14} & \Lambda_{15} & 0 \\ * & \Lambda_{22} & \Lambda_{23} & \Lambda_{24} & \Lambda_{25} & 0 \\ * & * & \Lambda_{33} & \Lambda_{34} & 0 & 0 \\ * & * & * & \Lambda_{44} & \Lambda_{45} & 0 \\ * & * & * & * & \Lambda_{55} & 0 \\ * & * & * & * & * & \Lambda_{66} \end{bmatrix} < 0, \tag{3.10}$$

where

$$\begin{aligned}
&\Lambda_{11} = 2\tilde{A} \otimes \bar{R} + \mathscr{I}_6 \otimes \mathcal{J}_2 + \bar{Q}_3 - \bar{Z}_3), \mathcal{J}_2 = J_{i,h}(R) = \textstyle\sum_{(j,k)\neq(i,h)} q_{(i,h),(j,k)}(R_{j,k} - R_{i,h}),\\
&\mathscr{I}_6 = \mathrm{diag}\{I_{n-1}, I_{n-m}\}, \Lambda_{12} = -A_r \otimes \bar{K} + \mathscr{I}_6 \otimes (\bar{Z}_3 - \bar{Z}_4), \Lambda_{13} = \mathscr{I}_6 \otimes \bar{Z}_4, \Lambda_{14} = B_r \otimes \bar{K},\\
&\Lambda_{15} = \tilde{A} \otimes \bar{R}, \Lambda_{22} = \mathscr{I}_6 \otimes (-2\bar{Z}_3 + \bar{Z}_4 + \bar{W}_4^{\mathrm{T}} + \lambda\bar{\Phi}_1), \bar{\Phi}_1 = \mathrm{diag}\{\sigma_1\bar{\Omega}_1, \sigma_2\bar{\Omega}_2, \sigma_3\bar{\Omega}_3\},\\
&\Lambda_{23} = \mathscr{I}_6 \otimes (\bar{Z}_3 - \bar{Z}_4), \Lambda_{25} = -A_r \otimes \bar{K}, \Lambda_{33} = -\mathscr{I}_6 \otimes \{\bar{Q}_3 + \bar{Z}_3\}, \Lambda_{44} = -\mathscr{I}_6 \otimes \lambda\kappa\bar{\Phi}_2,\\
&\bar{\Phi}_2 = \mathrm{diag}\{\bar{\Omega}_1, \bar{\Omega}_2, \bar{\Omega}_3\}, \Lambda_{45} = B_r \otimes \bar{K}, \Lambda_{55} = \mathscr{I}_6 \otimes (\vartheta^2\tau_M^{-2}\tilde{Q}_4 - 2\vartheta\bar{R}), \Lambda_{66} = -\mathscr{I}_6 \otimes \lambda\bar{\Phi}_2,
\end{aligned}$$

then consensus error system (2.23) is stable (and consequently, HMASs can achieve consensus), and satisfies the predefined performance. Moreover, the consensus control gain can be obtained: $K = \bar{K}\bar{R}^{-1}$.

Proof. Consider the Lyapunov function as:

$$V_2(t, \sigma(t)) = e_c^{\mathrm{T}} R_{\sigma(t)} e_c + \int_{t-\tau_M}^{t} e_c^{\mathrm{T}}(\upsilon)\, Q_3 e_c(\upsilon)\, d\upsilon + \tau_M \int_{-\tau_M}^{0}\int_{t+\theta}^{t} \dot{e}_c^{\mathrm{T}}(\upsilon)\, Q_4 \dot{e}_c(\upsilon)\, d\upsilon d\theta. \tag{3.11}$$

The subsequent proof follows arguments similar to those used in the proof of Theorem 1. For brevity, the details are omitted.

According to the definitions of the estimation error and the consensus error of the prediction system, the consensus error system of the actual system can be obtained as:

$$e_a = e_c + \begin{bmatrix} C_n \otimes I_p & 0 \\ 0 & I_{(n-m)p} \end{bmatrix} e_i.$$

From Theorem 2, the global consensus error of the prediction system satisfies $\lim_{t\to\infty} e_c = 0$. From Theorem 1, the estimation error satisfies $\lim_{t\to\infty} e_i = 0$. Therefore, it can be obtained that $\lim_{t\to\infty} e_a = 0$. This completes the proof. □

Remark 4. *Theorems 1 and 2 address two complementary aspects of the resilient consensus problem. Specifically, Theorem 1 establishes the stability and performance of the augmented estimation error system, which characterizes the discrepancies between the actual and predicted states as well as the*

attack estimation errors. Theorem 2 investigates the global consensus behavior of the heterogeneous multi-agent system by constructing a unified consensus error vector that incorporates the position disagreements among all agents and the complete velocity states of the second-order agents. In particular, the global position disagreement explicitly accounts for both intra-group and inter-group position differences. Consequently, the asymptotic stability of the consensus error system guarantees that all agents achieve position agreement and that the velocities of all second-order agents converge to zero. Together, these two theorems establish the estimation performance and consensus properties of the considered HMASs under composite attacks and inconsistent semi-Markov switching topologies. The consensus conclusion for the actual system additionally requires the state estimation errors to vanish asymptotically.

4. Simulation study

The validity of the previous results will be illustrated in this section by a numerical example presented below.

Suppose that HMAS (2.1) consists of two first-order agents and two second-order agents, and that the communication topology among these agents is shown in Figure 2. Specifically, agents 1 and 2 are first-order agents, whereas agents 3 and 4 are second-order agents. The switching between the communication topologies $\mathcal{G}_1$ and $\mathcal{G}_2$ is governed by an inconsistent semi-Markov process. In addition, all edge weights in graph $\mathcal{G}$ are set to 1.

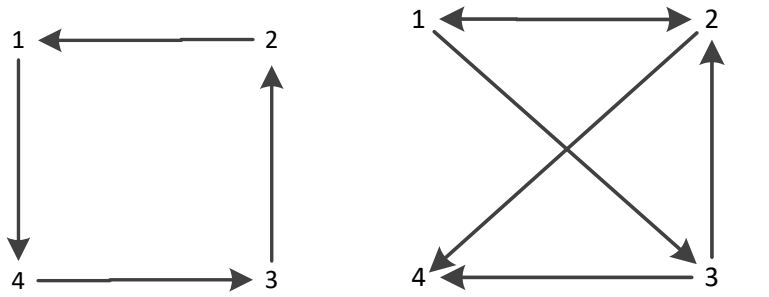

(a) Communication topology $\mathcal{G}_2$ **(b)** Communication topology $\mathcal{G}_2$

Figure 2. The communication topology $\mathcal{G}$ of HMASs.

Suppose that semi-Markov processes $\sigma_1(t)$ and $\sigma_2(t)$ both follow the Weibull distribution, namely, $T_i^{(q)} \sim \text{Weibull}(a_i^{(q)}, b_i^{(q)}), q \in \{1, 2\}$, and the probability density function for the residence time is

$$f_i^{(q)}(\tau) = \frac{b_i^{(q)}}{a_i^{(q)}} \left(\frac{\tau}{a_i^{(q)}} \right)^{b_i^{(q)}-1} \exp\left[-\left(\frac{\tau}{a_i^{(q)}} \right)^{b_i^{(q)}} \right],$$

where $a_i^{(q)} > 0$ is a scale parameter and $b_i^{(q)} > 0$ is a shape parameter. The corresponding hazard function is

$$S_i^{(q)}(\tau) = \exp\left[-\left(\frac{\tau}{a_{qi}} \right)^{b_{qi}} \right].$$

Consequently, the time-varying transition intensity from the current mode is determined by the hazard rate

$$\lambda_i^{(q)}(\tau) = \frac{f_i^{(q)}(\tau)}{S_i^{(q)}(\tau)} = \frac{b_{qi}}{a_{qi}}\left(\frac{\tau}{a_{qi}}\right)^{b_{qi}-1}.$$

Set the scale parameters of the semi-Markov process $\sigma_1(t)$ to $a_{11} = 1.0$, $a_{12} = 1.0$, and the shape parameters $b_{11} = 2.0$, $b_{12} = 2.0$. Accordingly, the transition intensities of the two processes can be expressed as

$$Q_1(\tau_1) = \begin{bmatrix} -2\tau_1 & 2\tau_1 \\ 2\tau_1 & -2\tau_1 \end{bmatrix}, Q_2(\tau_2) = \begin{bmatrix} -2.5 & 2.5 \\ 3.125\tau_2 & -3.125\tau_2 \end{bmatrix},$$

where τ_1 and τ_2 denote the elapsed sojourn times of the corresponding processes. These matrices describe the sojourn-time-dependent transition intensities of the two semi-Markov processes. In the simulations, the two processes are independently generated according to their respective Weibull sojourn-time distributions.

The resulting trajectories of the two semi-Markov processes are illustrated in Figure 3. It can be observed that the two processes exhibit different switching patterns owing to their distinct sojourn-time distributions and transition intensities. Furthermore, the global communication topology changes whenever either process switches its mode, thereby generating four possible joint switching configurations. This demonstrates that the proposed model can characterize the inconsistent stochastic switching behaviors of the two heterogeneous agent groups.

In addition, the conditional probabilities of semi-Markov process $\sigma_2(t)$ conditioned on semi-Markov process $\sigma_1(t)$ are given as follows: $p_{11} = 0.8$, $p_{12} = 0.2$, $p_{21} = 0.3$, $p_{22} = 0.7$. By taking these parameters, the semi-Markov process of the HMASs is shown in Figure 3, where the coordinate variables l and m express the mode at the current moment of the FO and SO agent.

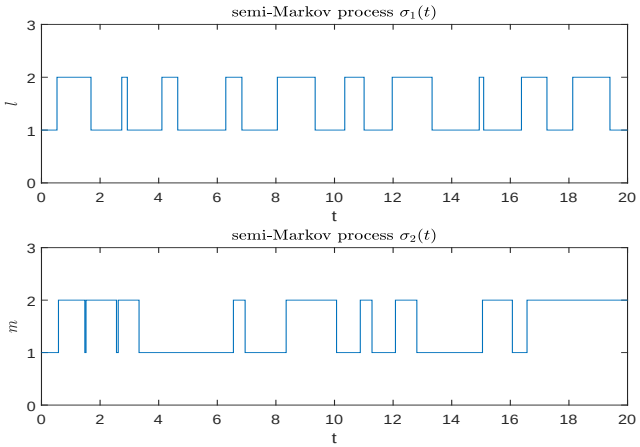

Figure 3. The considered semi-Markov processes in the HMASs.

Then, the initial state value for each agent is: $x_1(0) = [3; -4]$, $x_2(0) = [2; -1.5]$, $x_3(0) = [-1; 1]$, $x_4(0) = [3; -1]$, $v_3(0) = [-0.2; 0.1]$, $v_4(0) = [0.4; 0.7]$. Assume that the sensors and actuators of different agents in HMASs (2.1) are affected by attacks at different times. Specifically, the sensors and actuators of agents 1 and 2 are affected by the attack at 8.5 s, while those of agents 3 and 4 are affected at 9.0 s. For the first-order agents, the position sensor attacks are defined as $f_{x,11}(t) = f_{x,12}(t) =$

$0.1\cos(t)$ for $t \geq 8.5$ s, and as zero otherwise. For the second-order agents, the position and velocity sensor attacks are given by $f_{x,21}(t) = f_{x,22}(t) = f_{v,21}(t) = f_{v,22}(t) = 0.2\cos(t)$ for $t \geq 9.0$ s, and are zero otherwise. Meanwhile, the actuator deception attacks are introduced as $f_{u,11}(t) = f_{u,12}(t) = 0.1\sin(t)$ for $t \geq 8.5$ s, and $f_{u,21}(t) = f_{u,22}(t) = 0.1\sin(t)$ for $t \geq 9.0$ s, respectively, and are zero otherwise.

In addition, the considered ABETM relies on sample-data, and the sampling interval is $t_h = 0.1$ s. The parameters for ABETM-a are selected as: $\sigma_1 = 0.006$, $\sigma_2 = 0.008$, $\sigma_3 = 0.004$, $\Omega_1 = [22.41, 0; 0, 23.12]$, $\Omega_2 = [25.38, 0; 0, 28.21]$, $\Omega_3 = [15.43, 0; 0, 14.14]$. The parameters for event-triggered mechanism ABETM-b are $\sigma_4 = 0.0002$, $\sigma_5 = 0.006$, $\sigma_6 = 0.0001$, $\Omega_4 = [28.41, 0; 0, 25.12]$, $\Omega_5 = [15.24, 0; 0, 18.17]$, $\Omega_6 = [17.36, 0; 0, 19.45]$. Subsequently, the gain matrix is selected as:

$$k_1 = [1.52, 0.32; 0.32, 1.56], k_2 = [0.95, 0.13; 0.13, 0.97], k_3 = [1.96, 0.18; 0.18, 1.74],$$
$$k_1^x = [0.51, 0.12; 0.12, 0.52], k_2^x = [0.63, 0.09; 0.09, 0.68], k_3^x = [0.92, 0.14; 0.14, 0.86],$$
$$k_1^f = [0.74, 0.05; 0.05, 0.63], k_2^f = [1.23, 0.07; 0.07, 1.15], k_3^f = [1.65, 0.16; 0.16, 1.48].$$

By simulation, one can obtain Figures 4–9. Figures 4 and 5 show the evolution trajectories of the system states under no-attack conditions. It can be observed that the states of all agents gradually converge to a common trajectory, indicating that the system can achieve consensus under normal conditions. Therefore, the predictor can provide nominal state information for the attacked system, and its state trajectory can be regarded as the desired reference trajectory to be tracked by the attacked system. Figure 6 compares the actual state of the attacked system under the proposed control method with the state trajectory of the predictor. Here, the actual states denote the compensated responses of the system subject to attacks. As shown in Figure 6, under the proposed control method, the actual state of the attacked system maintains the normal state trajectory observed. This demonstrates that the proposed control method can effectively preserve consensus and stability even when the system is affected by attacks. Figure 7 illustrates the state trajectories of the HMASs without attack compensation. As can be observed, in the presence of sensor and actuator attacks, the states of the agents fail to converge to a common value in the absence of attack compensation. Moreover, the velocity states of the second-order agents do not converge to zero. This demonstrates that the proposed controller can effectively mitigate the effects of compound deception attacks and achieve system consensus.

Figure 8 illustrates the triggering moments of the position and velocity states under ABETM-a and ABETM-b, from which it is also seen that it is possible to reduce the data transmission. Table 1 compares the number of triggers for each agent between the event-triggered mechanism proposed in this paper and several other event-triggered mechanisms. As can be seen from Table 1, the designed event-triggering mechanism effectively reduces the number of triggers. As shown in Table 1, the proposed double ABETM generates an average of 34.0 triggering events, compared with 196.8 events under the conventional ETM, corresponding to an approximately 82.72% reduction. This result demonstrates that the proposed accumulated-error-based triggering strategy can effectively reduce unnecessary communication updates in the considered HMASs. Figure 9 represents the control inputs.

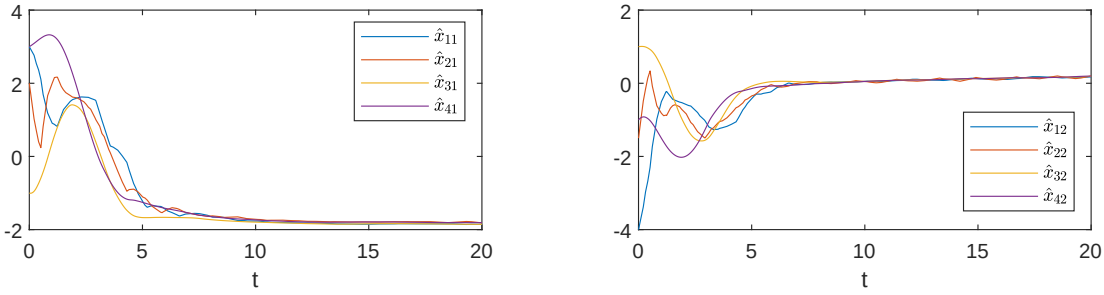

(a) **(b)**

Figure 4. Evolution curves of the position in the HMASs.

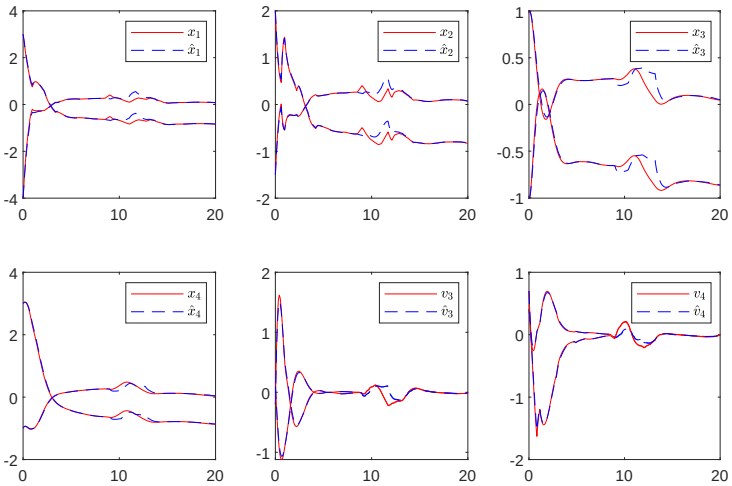

Figure 5. Evolution curves of velocity in the HMASs.

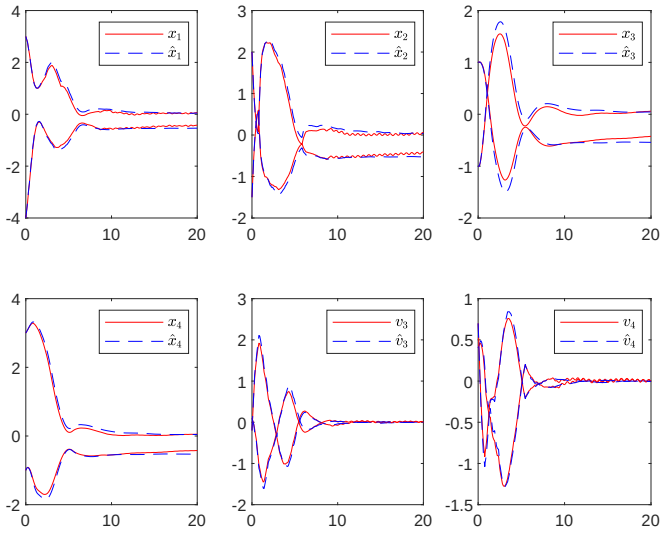

Figure 6. The estimation curve of the state (with attack compensation).

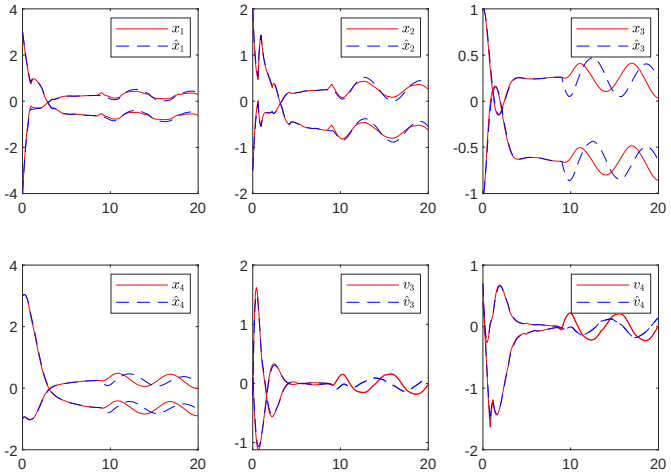

Figure 7. The estimation curve of the state (without attack compensation).

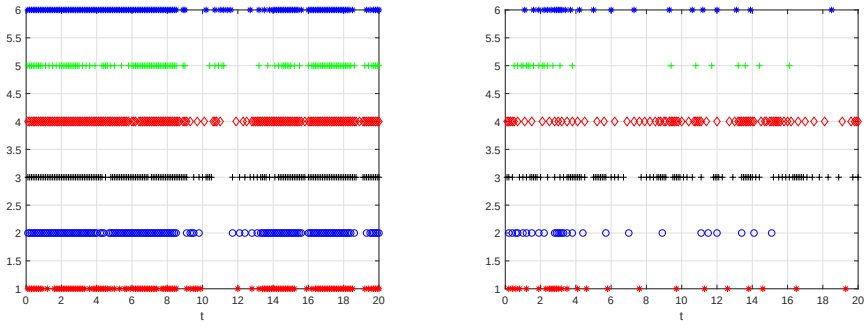

(a) ABETM-a **(b)** ABETM-b

Figure 8. Trigger moments of the ABETM.

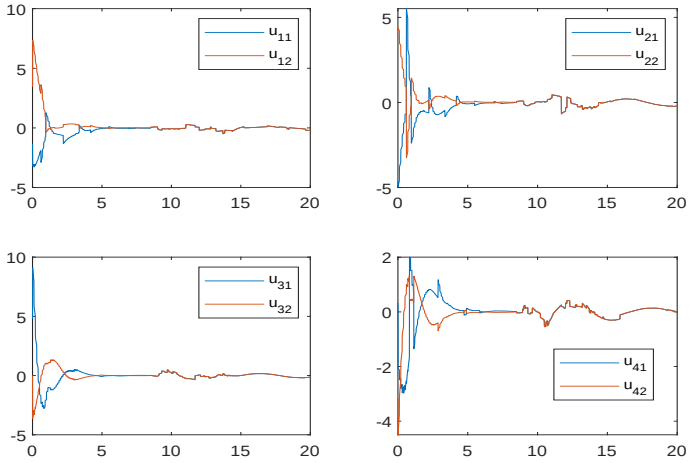

Figure 9. Control inputs.

Table 1. Comparison of ETMs.

	Trigger strategy type				
	ETM	Double ETM		Double ABETM	
		(ETMa)	(ETMb)	(ABETMa)	(ABETMb)
$x_1/\hat{x}_1$	197	195	63	77	29
$x_2/\hat{x}_2$	197	195	62	78	33
$x_3/\hat{x}_3$	198	187	151	74	39
$x_4/\hat{x}_4$	194	185	72	77	43
$v_3/\hat{v}_3$	198	187	60	92	31
$v_4/\hat{v}_4$	197	187	61	91	29
Average number of events	196.8	189.3	78.2	81.5	34.0

To evaluate the proposed double BAETM, four triggering strategies are compared: ETM-ETM, BAETM-ETM, ETM-BAETM, and BAETM-BAETM. All other simulation parameters and conditions are kept identical. Figure 10 shows the triggering instants under the four strategies. It can be observed that the proposed BAETM-BAETM generates fewer triggering events than the conventional ETM-ETM. As shown in Figure 11(a), the total triggering numbers of the four strategies are 1381, 1156, 999, and 693, respectively. Thus, the proposed double BAETM reduces the triggering number by 49.78% compared with the conventional ETM-ETM. By computing

$$e_p(t) = \sqrt{\frac{1}{6}\sum_{i=1}^{4}\sum_{j=i+1}^{4}\|x_i(t) - x_j(t)\|^2}, e_v(t) = \|v_3(t) - v_4(t)\|,$$

Figure 11(b) shows the position and velocity disagreement trajectories. All four strategies achieve consensus, exhibiting similar convergence behaviors. As reported in Table 2, the total consensus error integral of the proposed scheme is 18.9685, which is slightly lower than that of the conventional ETM-ETM (19.3474). These results demonstrate that the proposed double BAETM effectively reduces communication updates while maintaining comparable consensus performance.

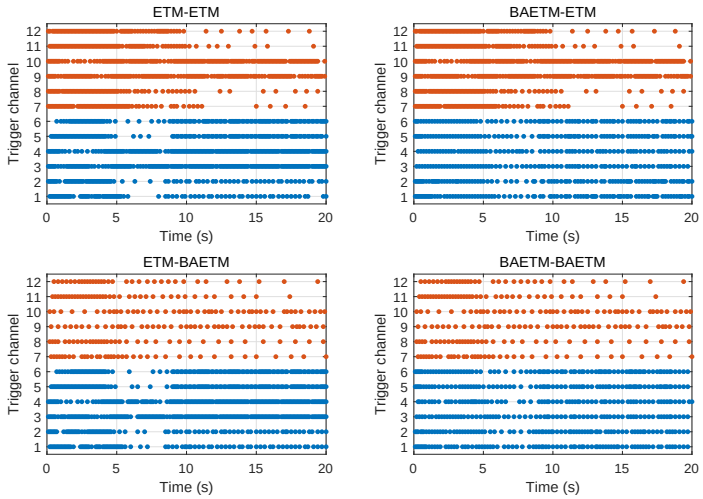

Figure 10. The triggering instants under different strategies.

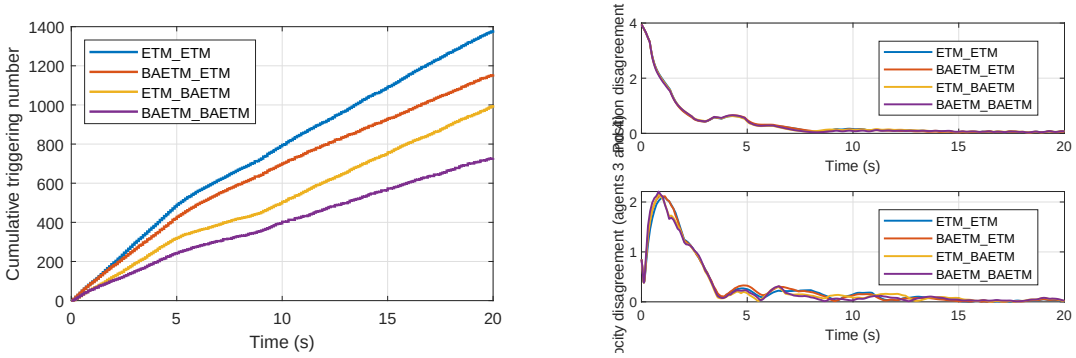

(a) The total triggering numbers **(b)** Position and velocity disagreement trajectories

Figure 11. Performance comparison of different strategies.

Table 2. Quantitative comparison of different ETMs.

Triggering mechanism	Number of triggering events			R_N (%)	Consensus error integral		
	N_A	N_B	N_{total}		J_{position}	J_{velocity}	$J_{\text{consensus}}$
ETM–ETM	746	635	1381	0	12.1527	7.1947	19.3474
BAETM–ETM	521	635	1156	16.29	12.0367	7.4983	19.5350
ETM–BAETM	761	238	999	27.66	12.0114	6.8959	18.9073
BAETM–BAETM	**489**	**204**	**693**	**49.78**	**11.8818**	**7.0867**	**18.9685**

Note: N_A and N_B denote the numbers of triggering events in ETM A and ETM B, respectively. $N_{\text{total}} = N_A + N_B$ represents the total number of triggering events. R_N denotes the reduction rate of triggering events relative to the conventional ETM–ETM scheme. J_{position} and J_{velocity} represent the integrals of the position and velocity disagreement errors, respectively, and $J_{\text{consensus}} = J_{\text{position}} + J_{\text{velocity}}$.

5. Conclusions

In this paper, the secure consensus for HMASs composed of first-order and second-order agents under inconsistent semi-Markov switching topologies and composite attacks is investigated. Inconsistent semi-Markov processes are employed to describe the topological switching behavior of first-order and second-order agents, respectively. To mitigate the impact of composite attacks involving both actuator attacks and sensor attacks, a predictor is designed to estimate the nominal states of the agents. Based on the estimated states and relative output errors, a resilient consensus controller is constructed to effectively suppress the effects of composite attacks. Furthermore, to reduce communication burden, an ABETM is developed to alleviate the influence of error fluctuations. By employing Lyapunov stability theory, the Kronecker product, and appropriate inequality techniques, sufficient conditions are derived to guarantee secure consensus of the system. Simulation results demonstrate that the proposed method achieves secure consensus under composite attacks while effectively reducing the number of triggering events.

Author contributions

Dongxiao Hu: Writing–review and editing, Formal analysis; Jiwei Gao: Methodology, Writing–review and editing, Formal analysis; Jianwei Ma: Supervision, Methodology, Writing–review and

editing; Shaofei Zang: Methodology, Writing–review and editing. All authors have read and approved the final version of the manuscript for publication.

Use of AI tools declaration

The authors declare that they have not used Artificial Intelligence (AI) tools in the creation of this article.

Acknowledgments

This work was supported by the Natural Science Foundation of Henan (No. 262300421788), National Natural Science Foundation of China (No. 62073124), and Key Scientific Research Projects of Universities in Henan Province (No. 27A120002).

Conflict of interest

All authors declare no conflicts of interest in this paper.

References

1. Y. H. Su, P. Bhowmick, A. Lanzon, A fixed-time formation-containment control scheme for multi-agent systems with motion planning: Applications to quadcopter UAVs, *IEEE T. Veh. Technol.*, **73** (2024), 9495–9507. http://doi.org/10.1109/TVT.2024.3382489
2. X. Wang, J. Wang, Y. Y. Chen, Y. Ma, S. Li, Hierarchical consensus of constrained second-order multi-agent systems with application to formation of multiple mobile robots, *IEEE T. Autom. Contr.*, **71** (2025), 886–901. http://doi.org/10.1109/TAC.2025.3602134
3. L. Wang, Z. Wang, K. Gumma, A. Turner, S. Ratchev, Multi-agent cooperative swarm learning for dynamic layout optimisation of reconfigurable robotic assembly cells based on digital twin, *J. Intell. Manuf.*, **36** (2025), 2959–2982. http://doi.org/10.1007/s10845-023-02229-7
4. A. A. Okine, N. Adam, F. Naeem, G. Kaddoum, Multi-agent deep reinforcement learning for packet routing in tactical mobile sensor networks, *IEEE T. Netw. Serv. Man.*, **21** (2024), 2155–2169. http://doi.org/10.1109/TNSM.2024.3352014
5. S. Huang, C. Sun, R. Q. Wang, D. Pompili, Toward adaptive and coordinated transportation systems: A multi-personality multi-agent meta-reinforcement learning framework, *IEEE T. Intell. Transp.*, **26** (2025), 12148–12161. http://doi.org/10.1109/TITS.2025.3560227
6. Z. Wang, C. Mu, S. Hu, C. Chu, X. Li, Modelling the dynamics of regret minimization in large agent populations: A master equation approach, *Proc. Int. Joint Conf. Artif. Intell. (IJCAI)*, (2022), 534–540. https://doi.org/10.24963/ijcai.2022/76
7. D. Zhang, Y. Hao, Q. Yuan, C. Qin, Dynamic event-triggered approximate optimal consensus control for unknown nonlinear multi-agent systems via adaptive dynamic programming, *ISA T.*, **172** (2026), 21–32. http://doi.org/10.1016/j.isatra.2026.03.010

8. Y. Zhou, G. Wen, G. Chen, Bipartite consensus tracking of heterogeneous multi-agent systems: A smooth output-feedback control approach, *Automatica*, **178** (2025), 112363. http://doi.org/10.1016/j.automatica.2025.112363
9. O. S. Oubbati, J. Alotaibi, F. Alromithy, M. Atiquzzaman, M. R. Altimania, A UAV-UGV cooperative system: Patrolling and energy management for urban monitoring, *IEEE T. Veh. Technol.*, **74** (2025), 13524–13536. http://doi.org/10.1109/TVT.2025.3563971
10. Y. Zhong, R. Ashfaq, A. Khan, A. U. K. Niazi, T. Saidani, A. B. Rajab, et al., Control protocol design for group consensus in heterogeneous multi-agent systems with communication interruptions and external disturbances, *AIMS Math.*, **10** (2025), 19750–19774. http://doi.org/10.3934/math.2025881
11. X. Li, J. Wu, X. Zhan, L. Cheng, Q. Yang, Robust neuro-adaptive bipartite formation control for nonlinear multi-agent systems subject to Markovian switching topologies and additive noise, *Neurocomputing*, **648** (2025), 130655. http://doi.org/10.1016/j.neucom.2025.130655
12. M. Meng, K. Xiang, Q. Gan, L. Chang, Event-triggered fixed-time consensus tracking of nonlinear delayed multi-agent systems with disturbances under switching topologies, *AIMS Math.*, **11** (2026), 20473–20501. http://doi.org/10.3934/math.2026833
13. X. Song, J. Man, C. Ki Ahn, S. Song, Finite-time dissipative synchronization for Markovian jump generalized inertial neural networks with reaction–diffusion terms, *IEEE Trans. Syst. Man Cybern. Syst.*, **51** (2021), 3650–3661. http://doi.org/10.1109/TSMC.2019.2958419
14. M. Svishchuk, A. V. Swishchuk, Stochastic optimal control of averaged SDDE with semi-Markov switching and with application in economics, *Mathematics*, **13** (2025), 1440. http://doi.org/10.3390/math13091440
15. S. Tian, H. Shen, H. Tian, Resilient consensus of nonlinear multi-agent systems with semi-Markov switching in unsecure environments under DoS attacks, *IEEE T. Signal Inf. Process. Netw.*, **12** (2026), 529–543. http://doi.org/10.1109/TSIPN.2026.3682187
16. M. Ban, J. Li, H. Deng, Y. Wang, J. Cheng, Dynamic event-triggered H_∞ leader-following consensus for nonlinear stochastic multi-agent systems with semi-Markov switching topologies and application, *J. Franklin Inst.*, **362** (2025), 107596. http://doi.org/10.1016/j.jfranklin.2025.107596
17. W. Cao, D. Zhang, G. Feng, Resilient semi-global finite-time cooperative output regulation of heterogeneous linear multi-agent systems subject to denial-of-service attacks, *Automatica*, **173** (2025), 112099. http://doi.org/10.1016/j.automatica.2024.112099
18. G. A. Usmani, M. Rehan, X. Wu, A. ur Rehman, Resilient consensus control for heterogeneous multi-agent systems subject to two-channel stochastic deception attacks, *IEEE T. Consum. Electron.*, **72** (2025), 2049–2060. http://doi.org/10.1109/TCE.2025.3645813
19. T. Y. Zhang, G. H. Yang, D. Ye, Asymmetrical vulnerability of heterogeneous multi-agent systems under false-data injection attacks, *Automatica*, **171** (2025), 111947. http://doi.org/10.1016/j.automatica.2024.111947
20. X. Wang, T. Huang, Optimized adaptive finite-time consensus control for stochastic nonlinear multiagent systems with non-affine nonlinear faults, In: *Optimal Adaptive Cooperative Control for Nonlinear Multiagent Systems, Springer Nature Singapore*, 2026, 159–184. https://doi.org/10.1007/978-981-95-2964-3_8

21. L. Xia, Q. Li, R. Song, L. Liu, Resilient output synchronization dynamic event-triggered control to link faults in heterogeneous multi-agent systems, *Int. J. Robust Nonlin.*, **34** (2024), 4736–4752. http://doi.org/10.1002/rnc.7225
22. Z. Li, K. He, Z. Yang, L. Lian, Y. Sun, H. Zhao, Two-layer game-based consensus security control for stochastic multiagent systems over sensor attacks, *AIMS Math.*, **11** (2026), 31185–31213. http://doi.org/10.3934/math.20261232
23. K. Li, C. Hua, X. You, Z. Xu, Distributed consensus of feedforward nonlinear stochastic multiagent systems subject to actuator attacks, *IEEE T. Cybern.*, **55** (2025), 4842–4851. http://doi.org/10.1109/TCYB.2025.3597979
24. Z. Chen, Z. Yu, S. Li, Output feedback adaptive inverse optimal security control for stochastic nonlinear cyber-physical systems under sensor and actuator attacks, *Nonlinear Dyn.*, **112** (2024), 19243–19259. http://doi.org/10.1007/s11071-024-10043-w
25. V. S. Dolk, K. J. A. Scheres, R. Postoyan, W. P. M. H. Heemels, Time- and event-triggered communication for multi-agent systems–Part I: General framework, *IEEE T. Autom. Contr.*, **70** (2024), 447–462. http://doi.org/10.1109/TAC.2024.3427908
26. X. Wang, N. Pang, Y. Xu, T. Huang, J. Kurths, On state-constrained containment control for nonlinear multiagent systems using event-triggered input, *IEEE Trans. Syst. Man Cybern. Syst.*, **54** (2024), 2530–2538. http://doi.org/10.1109/TSMC.2023.3345365
27. D. Wang, Z. Yuan, A. Liu, Q. Hu, J. Qiao, Static and dynamic event-triggered control for disturbed interconnected systems through adaptive critic designs, *IEEE T. Syst. Man Cybern. Syst.*, **56** (2025), 878–892. http://doi.org/10.1109/TSMC.2025.3638702
28. Y. Ma, Z. Hu, X. Qi, S. Hu, X. Xie, Y. Zhao, et al., Dynamic event-triggered fuzzy control of networked unmanned surface vehicles under hybrid cyber attacks, *IEEE T. Ind. Electron.*, **72** (2024), 6422–6431. http://doi.org/10.1109/TIE.2024.3497323
29. M. Long, H. Su, W. X. Zheng, Y. Wang, R. Su, Adaptive event-triggered distributed observer for unknown-input LTI systems, *IEEE T. Autom. Contr.*, **70** (2025), 8274–8281. http://doi.org/10.1109/TAC.2025.3581142
30. X. M. Zhang, Q. L. Han, B. L. Zhang, X. Ge, D. Zhang, Accumulated-state-error-based event-triggered sampling scheme and its application to H_∞ control of sampled-data systems, *Sci. China Inf. Sci.*, **67** (2024), 162206. http://doi.org/10.1007/s11432-023-4038-3
31. J. Zhao, H. Zhao, Y. Song, Z. Y. Sun, D. Yu, Fast finite-time consensus protocol for high-order nonlinear multi-agent systems based on event-triggered communication scheme, *Appl. Math. Comput.*, **508** (2026), 129631. http://doi.org/10.1016/j.amc.2025.129631
32. Z. Shen, L. Zhang, N. Zhao, Reachable set synthesis of nonlinear heterogeneous multi-agent systems with Markov switching topologies, *J. Franklin Inst.*, **362** (2025), 107770. http://doi.org/10.1016/j.jfranklin.2025.107770
33. G. Liu, Q. Sun, H. Su, Z. Hu, Adaptive tracking control for uncertain nonlinear multi-agent systems with partially sensor attack, *IEEE T. Autom. Sci. Eng.*, **22** (2024), 6270–6279. http://doi.org/10.1109/TASE.2024.3440394
34. X. Li, G. Wen, Y. Lv, C. Sun, M. M. Polycarpou, Output consensus tracking of heterogeneous open multi-agent systems under actuator attacks, *IEEE T. Control Netw. Syst.*, **13** (2025), 423–435. http://doi.org/10.1109/TCNS.2025.3648473

35. C. Fan, L. Su, K. Wang, X. Fei, Event-triggered synchronization control for Markov jump neural networks with partially unknown transition probabilities, *Int. J. Robust Nonlin.*, **35** (2025), 2091–2100. http://doi.org/10.1002/rnc.7781

36. S. Vong, X. Ma, Y. Zhang, X. Han, Improved reciprocally convex cubic matrix inequalities for neural networks with time-varying delay, *J. Franklin Inst.*, **362** (2025), 107930. http://doi.org/10.1016/j.jfranklin.2025.107930

37. S. Jenhani, H. Gritli, An LMI-based robust state-feedback controller design for the position control of a knee rehabilitation exoskeleton robot: Comparative analysis, *Meas. Control*, **57** (2024), 1326–1346. http://doi.org/10.1177/00202940241236295

38. J. Yang, J. Wang, D. Shen, Observer-based sampled-data event-triggered tracking for nonlinear multi-agent systems with semi-Markovian switching topologies, *Inf. Sci.*, **676** (2024), 120803. http://doi.org/10.1016/j.ins.2024.120803

39. X. Yin, D. Yue, S. Hu, Adaptive periodic event-triggered consensus for multi-agent systems subject to input saturation, *Int. J. Control*, **89** (2016), 653–667. http://doi.org/10.1080/00207179.2015.1088967



AIMS Press

© 2026 the Author(s), licensee AIMS Press. This is an open access article distributed under the terms of the Creative Commons Attribution License (https://creativecommons.org/licenses/by/4.0)